

Morphological control in solvothermal synthesis of titanium oxide

Rong-Cai Xie · Jian Ku Shang

Received: 1 September 2006 / Accepted: 5 January 2007 / Published online: 30 April 2007
© Springer Science+Business Media, LLC 2007

Abstract A solvothermal method is described for preparing nanomaterials of titanium oxide with different morphologies. Nanostructures, such as wire, rod, cube, and fiber, were synthesized in mass quantities by controlling either the concentrations of the precursor or growth temperature and introducing different additives in one simple system based on titanium tetroisopropoxide and ethylene glycol. Hydrothermal treatment of the base system produced nanowires with diameters around 40 nm. The addition of ethylenediamine (EDA) to the system inhibited the radial expansion of the nanowires, resulting in nanorods and nanofibers with diameters down to about 2 nm. Increasing the EDA concentration tended to induce meso-scale self-assembly of nanofibers into arrays. The presence of water promoted the formation of nearly spherical nanoparticles with sizes dependent on the EDA concentration. At higher temperatures, the same system yielded well-defined nanobelts or nanocubes. The replacement of EDA by 2,4-pentanedione favored the formation of nanosheets while tetramethylammonium hydroxide appeared to confuse the growth of nanorods, creating a continuous network.

Introduction

Nanoparticles of titanium oxide have received great attention recently for their potential applications in catalysis [1], photocatalysis [2–4], dye-sensitized solar cells [5–7], water splitting [8, 9], and TiO₂-oligonucleotide nanocomposite for gene therapy [10, 11]. Since the physical and chemical properties of the semiconductor nanoparticles are strongly dependent on their size, shape, crystallinity, controlling the size and shape of titanium oxide is a key step in obtaining interesting properties. For instance, in TiO₂-based photocatalysts, the photo-induced electrons (e⁻) and holes (h⁺) tend to migrate to the TiO₂ surface to induce surface redox process. In spherical crystals, the benefits arising from higher surface-to-volume ratio with decreasing the particle size are significantly offset by the increased e⁻/h⁺ recombination probability at surface defect [12]. On the other hand, the increased delocalization of carriers in nanowires or rods, where they are free to move throughout the length of the crystal, is expected to greatly decrease the probability of recombination on the heterogeneous interface and improve the overall photoactivity [13]. Between the size and shape of nanoparticles, theoretical calculation shows that the shape of a semiconductor nanocrystal provides greater flexibility in increasing the variety of electronic states than simply reducing the size of the system [14].

So far only a few studies have reported synthetic pathways for controlling morphology of TiO₂ nanocrystals. In sol-gel template method, TiO₂ nanofibril or tubule was obtained in the pore of the membrane template [15]. While the use of a physical template can ensure a good control over the morphology, it complicates the synthetic procedure and limits the scale at which the crystal can be grown in each synthesis. More importantly, it is not appropriate for preparing small nanotube or nanorod because of the

Rong-Cai Xie—Formerly with the University of Illinois at Urbana-Champaign.

R.-C. Xie
Institute of Metal Research, Shenyang National Laboratory
for Materials Science, Shenyang 110016, China

J. K. Shang (✉)
Department of Material Science and Engineering,
University of Illinois at Urbana-Champaign, Urbana,
IL 61801, USA
e-mail: jkshang@uiuc.edu

large mold. To address this limitation, direct, chemical methods have recently been demonstrated for tuning TiO₂ morphologies. By hydrothermal method, the rutile nanorods were grown in acidic media [16], but the rutile form of TiO₂ is considered less active than the anatase in photocatalysis. Elongated TiO₂ nanocrystals [17], pseudocubic or ellipsoidal nanoparticles with varying aspect ratios (8–100 nm in diameter and 20–200 nm in length) have been synthesized in aqueous media or in alkaline solution [18, 19]. However, the chemisorbed and physisorbed water has significant effects on the properties of nanoscale oxides [20]. Synthesis of needle-shaped TiO₂ crystals with a diameter of 8 nm and a length of 100 nm was reported when TiO₂ powders or precursors were treated chemically with 5–10 M NaOH aqueous solution. Unfortunately, the chemical reaction led to formation of complex titanates, such as Na_xH_{2-x}Ti₃O₇, not TiO₂ [21]. Therefore, morphological control of anatase TiO₂ remains a serious challenge.

Recent developments in the synthesis of CdS and CdSe nanocrystals by rapid thermal decompositions of molecular precursors in the presence of strong coordinating agents has been extended to synthesize TiO₂ nanorod or diamond structure using carboxylic acid as the selective agent or trioctylphosphine oxide as the nonselective agent [12, 20, 22]. However, the problem with these high-temperature solvents, apart from their toxicity, is their high costs, which make scale-up non-viable. In the 1980s, Fievet et al. used ethylene glycol as a solvent and reducing agent for the preparation of submicrometer particles of the transition metals. This method, known as the *polyol* process [23], have been widely used in the preparation of nanowires such as Ag nanowire [24b], SnO₂ nanowire [25] and other metal oxide (including TiO₂, In₂O₃, PbO) nanowires [26, 27]. The potential of this kind of methods is, however, limited because of the requirement that the TiO₂-based nanomaterials must be produced at relatively large scale for the application as photocatalyst or solar cell materials. Moreover, the diameter of TiO₂ was still too large. Synthetic method is still needed to produce TiO₂ nanostructured materials in copious quantities with well-controlled dimension, morphology and crystallinity.

Solvothermal technique (especially the hydrothermal method) is widely used in the synthesis of the nanoparticles. Unlike most other synthetic processes, the solvothermal synthesis involves much milder conditions and softer chemistry conducted at relatively lower temperatures. Compared to those methods which require calcination and milling, such as sol-gel, coprecipitation, and solid state reactions, which tend to result in agglomerate formation and degradation of the surface, hydrothermal processing maintains the particles in solution throughout the process so that non-aggregated nanomaterials may be obtained readily. Here we describe a hydrothermal/

solvothermal method for preparing TiO₂ anatase nanocrystals or TiO₂ nanoparticles with controlled size and shape. The method was based on a single system in which morphological control was achieved by adjusting either the concentrations of precursors or growth temperature or additives. This method was used to synthesize TiO₂ nanofibers, self-assembly TiO₂ nanofiber, TiO₂ nanorod, TiO₂ nanobelt, TiO₂ nano network, TiO₂ nanosheet and TiO₂ nanoparticles in large quantity.

Experimental

Chemicals and materials

Reagent grade titanium tetrakisopropoxide (TTIP 98+%), tetramethylammonium hydroxide (TMA, 25% in methanol), ethylenediamine (EDA), ethylene glycol (EG), 2,4 pentanedione, and ethanol were purchased from Aldrich. These reagents were used as received without further purification.

Preparing TiO₂ nanostructured powders

In a typical reaction, 50 mL of EG was dried at 140 °C for 1 h under vigorous stirring in a flask under nitrogen atmosphere. After dehydrated with MgSO₄, the appropriate additive was added into EG and the mixture was stirred for 5 min. Then, an appropriate amount of Ti(OR)₄ was added into the above-mentioned mixture and the mixture was stirred for another 5 min. Immediately, the feedstock of 50 mL was transferred to a teflonlined stainless steel autoclave apparatus. The hydrothermal preparations were conducted in the temperature range 205–240 °C for 5–12 h at ambient pressure. After the autoclave was cooled to room temperature, the products were filtered and washed with ethanol for three times to remove excess solvent and additives.

Characterizing TiO₂ nanostructured powders with TEM and XRD

The TiO₂ nanoparticles were characterized by a JEOL 2010F electron microscope at an operating voltage of 200 kV. TEM samples were made by first suspending nanoparticles in ethanol, followed by dispersing the suspension on a holey carbon film supported by a copper grid.

The crystal structure of the particles was determined by X-ray Diffraction (XRD). XRD measurements were conducted with Rigaku D-Max X-ray diffractometer using a Cu target at an accelerating voltage of 45 kV and an emission current of 20 mA.

Results and discussion

Influence of the EDA concentration on the morphology of TiO₂

About 0.7 mL TTIP dissolved in 50 mL EG was heated to 205 °C and kept at this temperature for 12 h, until some gel precipitants were produced. After cooling down to room temperature, the precipitants were centrifuged, washed and dried. The resulting white powders were collected for further characterization. The TEM image of the powders obtained from this procedure is shown in Fig. 1a, where TiO₂ appeared as long solid wires. The diameters of the wires were relatively uniform, around 40 nm. The average length was about 5 μm. In this base system, EG apparently suppressed the hydrolysis of TTIP and served as a structure-directing agent due to the formation of linear polymer chains with relatively high molecular weights in the solution.

As a ligand to Ti atom, EDA was added to the base system to restrict TiO₂ growth. The effect of EDA was strongly dependent on its relative concentration. At very low concentrations, EDA only reduced the size of the

anatase crystal but the linear form of TiO₂ remained. Figures 1b and c show highly dispersed TiO₂ nanowires produced when 0.05 mL EDA and 0.10 mL EDA were added to the TTIP–EG system. The diameters of TiO₂ nanowires were decreased to 30 nm and 22 nm respectively. Further increase of EDA concentration to 0.3 mL led to a decrease in diameter to about 5 nm and length to 30 nm (Fig. 1d), turning long nanowires into short nanorods. Similarly, when EDA volume was less than 0.3 mL, a higher TTIP concentration yielded thicker nanowires with random morphologies.

It is well known that solvent plays an important role in determining the crystal morphology. Solvents with different physical and chemical properties can influence the solubility, reactivity, and diffusion behavior of the reactants, in particular, the polarity and coordinating ability of the solvents can influence the crystal morphology of the final product. EDA is widely used as a chelating ligand in inorganic chemistry. When mixed with the TTIP–EG base system, ethylenediamine should interact strongly with TTIP to form the complexes of ethylenediamine with titanium. The complexes may serve as surface modifiers to inhibit the radical enlargement of rods.

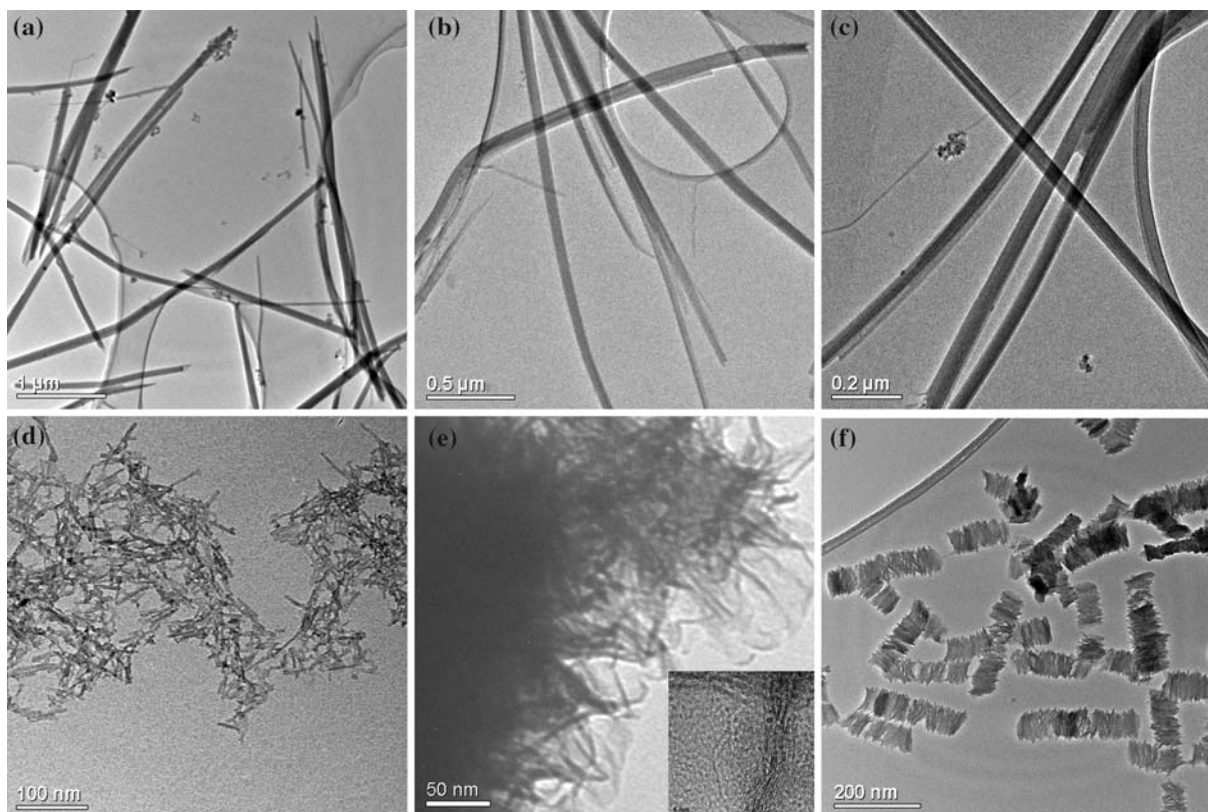


Fig. 1 TEM images of TiO₂ nanomaterials in EG–DEA system: (a) 40 nm, (b) 30 nm, and (c) 22 nm diameter wires, (d) 5 nm diameter rods, (e) 2 nm diameter fibers, and (f) nanofiber arrays

When the EDA concentration far exceeded the amount of TTIP, TiO_2 assumed a fine fibril form. The fibrils were much thinner than nanorods and tended to organize into an aggregated structure. Figure 1e shows TiO_2 fibers made by dissolving 2.84 mL TTIP in the mixture of 10 mL EDA with 50 mL EG. As shown by the high resolution TEM image in the insert, the diameter of a typical fiber varied from 1.5 to 2.5 nm along the length. The fibers were bundled together to form an entanglement about 60 nm. At a slightly higher EDA concentration (TTIP:EDA ratio of 1.0 mL: 5 mL), TiO_2 nanofibers were organized by mesoscale self-assembly into ordered arrays, as shown in Fig. 1f. The mesoscale ordering may be considered as a balance of the organic interactions at the interfaces between the hybrid building blocks and the stabilizing effect of EDA. As the concentration of EDA was increased relative to a fixed particle concentration, the formation of order structure becomes more favorable than the formation

of isolated or aggregated nanofibers [28]. The thermodynamic stability of this ordered structure apparently arises from a gain in translational entropy that overrules the loss of orientational entropy associated with particle alignment.

The effects of EDA concentration are summarized in Table 1, where the amount of the EG solvent was fixed at 50 mL. As the relative concentration of EDA increased, TiO_2 growth became more restricted, resulting in a finer linear nanostructure.

Influence of temperature on the morphology of TiO_2

The reaction temperature is also a key factor in the formation and assembly of the TiO_2 nanoparticles. When the hydrothermal temperature was lower than 170 °C, TiO_2 nanomaterials could not be formed, presumably because the Ti–amine–EG complex was too stable to be decomposed into TiO_2 nanoparticles.

While TiO_2 tended to form 1-D nanostructures at 205 °C, 1-, 2- and 3-D structures were produced by increasing the reaction temperature. For a small temperature increase to 220 °C, at the same reaction time of 12 h, 1-D nanowires were still the predominant structure as shown in Fig. 2a, but the nanowires tended to aggregate onto “strands” with random orientations. This may have formed because of the enhanced mobility of the nanowires

Table 1 Summary of TiO_2 nanostructures made with various EDA concentrations

TTIP/EDA	0	14	7	2	0.3	0.2
Structure	Wire	Wire	Wire	Rod	Fibers	Fibers

Note: Fiber is distinguished from wire here for its non-uniform diameter and high local curvature

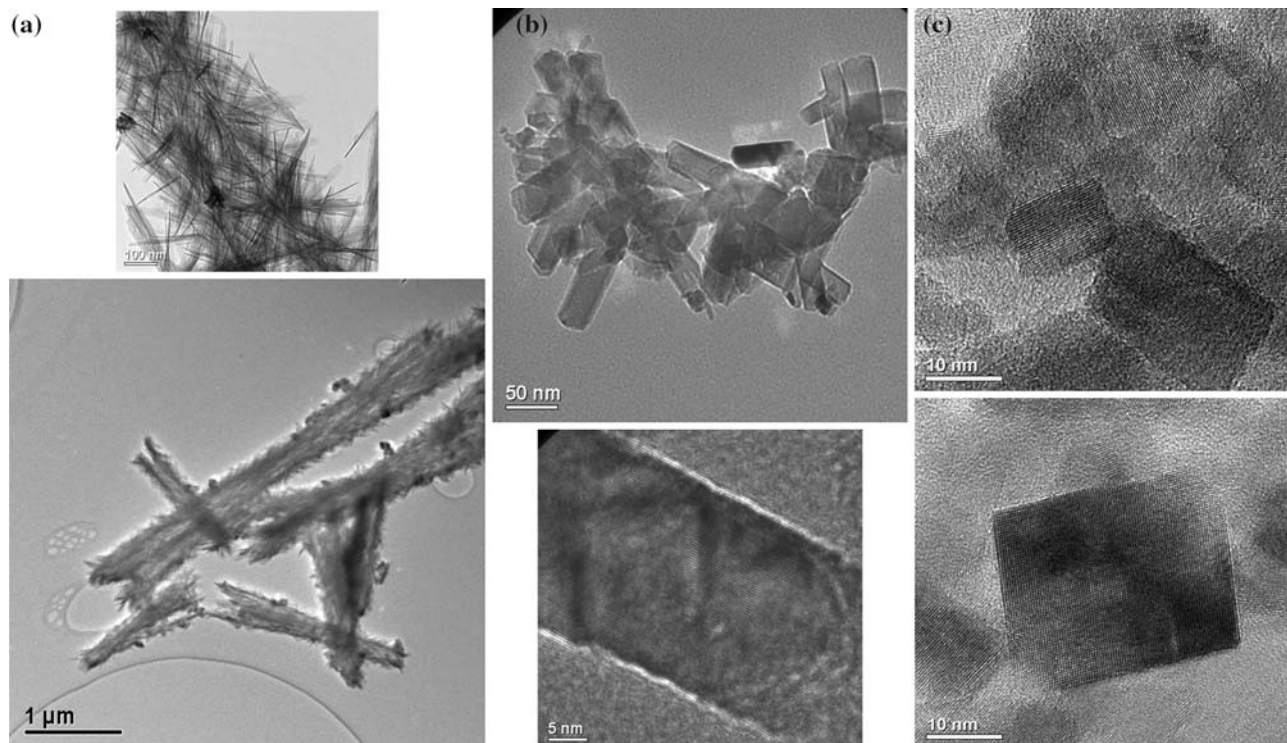


Fig. 2 TEM images of TiO_2 nanomaterials in EG–EDA system at higher temperatures: (a) strands of nanofibers, (b) “nanocards”, and (c) “nanotubes”

and the increased solubility of TTIP in EG–EDA solution at the higher temperature. The latter reduces the amount of TTIP to feed the nanowire growth, limiting the wires to very fine dimensions.

When the temperature was increased to 240 °C, both 2-D and 3-D morphologies were observed, depending on TTIP vs. EDA concentrations. At a high TTIP:EDA concentration ratio of 10 (1 mL TTIP dissolved in the mixture of 0.1 mL of EDA with 50 mL EG), heating to 240 °C for 12 h resulted in card-like structures, roughly 20 nm wide and 70 nm long, as shown in Fig. 2b. The “nanocards” tended to stack together into an aggregate. The stacks were highly transparent to the electron beam in the TEM, indicating that the “cards” were very thin. From the lattice fringes in Fig. 2b, the face of the nanocard was {001} plane of anatase TiO₂.

The 2-D structure above was extended to 3-D if the EDA concentration was far greater than TTIP. When 2.84 mL TTIP dissolved in the mixture of 10 mL EDA with 50 mL EG was heated to 240 °C for 12 h, a highly crystalline structure emerged as shown in Fig. 2c. In the high resolution TEM image, three distinct shapes were evident: a square, a rectangle, and parallelogram. Based on lattice fringes, these areas were identified as (001), (101), and {101} planes of the tetragonal anatase structure. Therefore, the high temperature synthesis produced nearly cubic structures. The edges of the cubes ranged from 5 nm to 22 nm. At this temperature, the kinetics of the TiO₂ crystal growth was efficient so that the shape of the crystal was determined by the minimization of the surface energy.

Influence of other ligands and water on the morphology of TiO₂

With replacement of EDA by TMA, 0.56 mL TTIP dissolved in the mixture of 3.5 mL TMA with 50 mL EG was heated to 205 °C and kept at this temperature for 12 h. The TEM picture in Fig. 3a shows that the precipitate is a nano

network with the diameter 5 nm. The OH groups in TMA may have attached on the TiO₂ surface and modified the oriented attachment mechanism by changing the surface energy and also preventing contact between the faces on which adsorption has selectively occurred. They may act as bridges across the nanorods to confuse the nanowire and form TiO₂ network system. Since the defects in the grain boundaries of the network may act as electron traps, such a network structure of TiO₂ is expected to result in a great improvement for rapid electron transfer and higher photocatalytic efficiency.

Similarly, by adopting another additive, 2,4-pentanedione, which is commonly used as chelating agent for making TiO₂ thin film, 0.56 mL TTIP dissolved in the mixture of 10 mL 2,4-pentanedione with 50 mL EG was heated to 205 °C and kept at this temperature for 12 h. The TEM picture is in Fig. 3b. The precipitate was a roll-like nanosheet interlaced like a cluster of crumpled paper. The nanosheet was measured 150 nanometer wide with a thickness of several nanometers. At this time, we do not have a clear explanation for how 2,4-pentanedione induces TiO₂ nanosheet. One possible explanation is that 2,4-pentanedione may help form TiO₂ nanosheet by exfoliation TiO₂ nanoparticles as 2,4-pentanedione intercalates the TiO₂ layers to form exfoliated titanate.

Because EG promotes the formation of TiO₂ nanowire while 2,4-pentanedione favors the titanium oxide layers, the combined effect is that the sheet of titanium oxide is curled to thin curled flakes. The flakes were not completely separated but assembled loosely like a flower.

When 0.64–1.28 mL water was added to the mixture of EDA (0.39 mL), TTIP (3 mL) system, nanoparticles with diameters of 5–7 nm were produced, as shown in Fig. 4a. Again because EDA slows crystal growth, increasing the EDA amount to 3 mL resulted in finer nanoparticles of 1.5–2.5 nm in size (Fig. 4b). The presence of water surrounding the nanoparticle surfaces is expected to induce massive precipitation of amorphous TiO₂ accompanied by

Fig. 3 TEM images of TiO₂ nanomaterials in EG–TMA (a) and 2,4-pentanedione (b) system

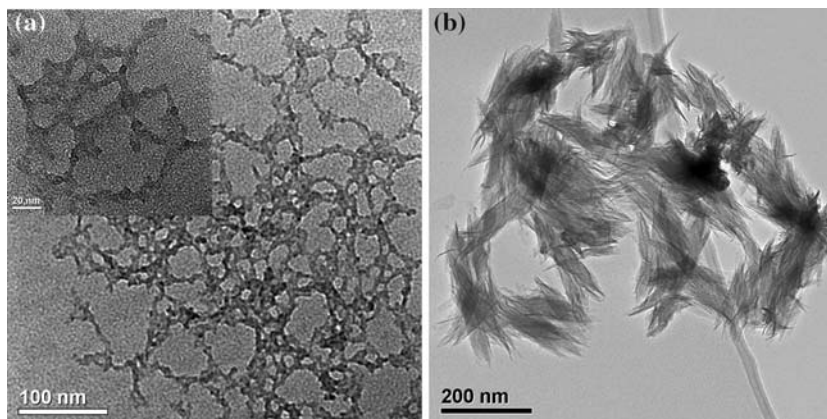
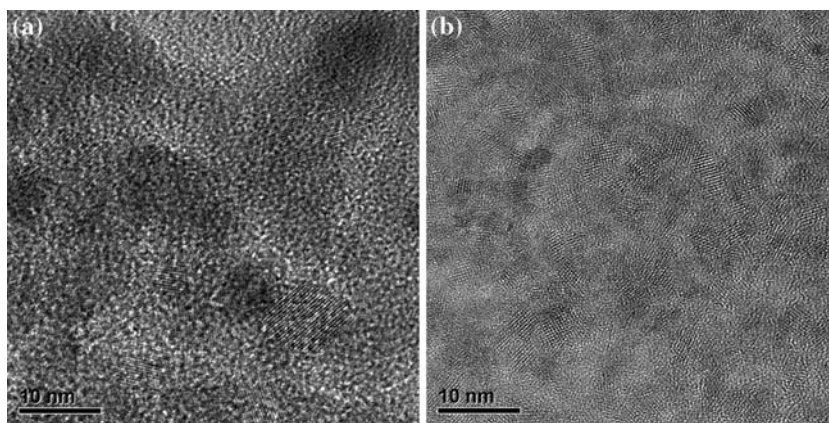


Fig. 4 TEM images of TiO₂ nanomaterials in EG–EDA–H₂O system: (a) 5–7 nm and (b) 2 nm particles



uncontrolled branching of the resulting Ti–O–Ti network, as hydrolysis and condensation are very fast and proceed at once. Under these conditions, particle growth is most likely governed by kinetics rather than by thermodynamics. So the presence of a small amount of water reduced the anisotropy in TiO₂ growth. Since hydrolysis–condensation rate in all growth directions is similar, the product should be an equiaxed particle.

Electron diffraction data of TEM show that all powders made at the lower temperatures (205 °C) were amorphous, except for 2 nm TiO₂ nanofiber. The crystallinity of the TiO₂ nanomaterials was conformed by XRD. Figure 5 presents the XRD patterns of nanocubic structure, nanosheet, 2 nm nanofiber and 2 nm nanoparticles. All diffraction peaks could be attributed to anatase (JCPDS no. 21-1272). The strong peak at 25.8° corresponds to anatase {101}. From the peak positions and their relative intensities, it was evident that no other phase of TiO₂ such as rutile and brookite was formed. As expected, the widths of individual diffraction peaks increased with decreasing particle size.

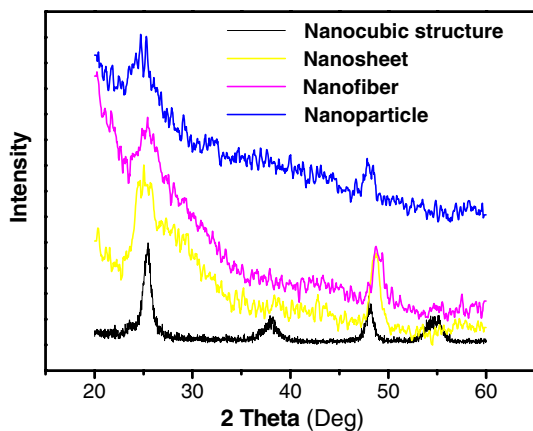


Fig. 5 XRD Patterns of TiO₂ of different morphologies

It is noted that formation of very fine TiO₂ crystallites, such as 2 nm nanoparticles and 2 nm nanofibers, was faster than that of bulk crystals. The enhanced crystallization rate is apparently related an appreciable amount of atomic vacancies and dangling bonds (both Ti and O) in its amorphous network in the very small system. The enhanced atomic diffusion during crystallization of the amorphous TiO₂ is likely to proceed through movement of the vacancies and the dangling bonds, leading to an accelerated crystallization.

Conclusion

Hydrothermal synthesis was carried out to make titanium oxide crystals of various morphologies. The synthetic strategy began with 1-D nanowire structure from a base system of TTIP and EG. Using EDA as a growth inhibitor, thinner wires, rods and fibers were made by adjusting the relative EDA concentration with respect to TTIP content. At very high EDA concentration, the excess EDA induced mesoscale ordering of nanofibers. By increasing temperature, 2-D and 3-D nanostructures were synthesized as the crystal strived to minimize its surface energy. Card-like 2-D nanostructure was produced at low EDA concentration while 3-D tetragonal nanostructure emerged from high EDA loading. The presence of a small amount of water promoted isotropic crystal growth, resulting in equiaxed nanoparticles.

Acknowledgements This study was supported by the Center of Advanced Materials for the Purification of Water with Systems, National Science Foundation, under Agreement Number CTS-0120978 and by the National Basic Research Program of China through Grant No. 2006CB601201. Characterization was carried out in CMM and LSF centers at the Frederick Seitz Materials Research Laboratory, University of Illinois at Urbana-Champaign, which is partially supported by the U.S. Department of Energy under grant DEFG02-91-ER45439.

References

1. Hadjiivanov KI, Klissurski DG (1996) *Chem Soc Rev* 25:61
2. Anpo M, Takeuchi M (2003) *J Catal* 216:505
3. Fujishima A, Rao TN, Tryk DA (2000) *J Photochem Photobio C: Photochem Rev* 1:1
4. Kaneko M, Okura I (2002) In: *Photocatalysis science and technology*, Kodansha, Springer
5. Bach U, Lupo D, Comte P, Moser JE, Weissortel F, Salbeck J, Spreitzer H, Gratzel M (1998) *Nature* 395:583
6. Gratzel M (2001) *Nature* 414:338
7. Zhang D, Yoshida T, Furuta K, Minoura H (2004) *J Photochem Photobio A: Chem* 164:159
8. Akikusa J, Khan SUM (2002) *Int J Hydrogen Energy* 27:863
9. Fujihara K, Ohno T, Matsumura M (1998) *J Chem Soc, Faraday Trans* 94:3705
10. Meier K, Gratzel M (2002) *Chemphyschem* 4:371
11. Paunescu T, Rajh T, Wiederrecht G, Master J, Vogt S, Stojicevic N, Protic M, Lai B, Oryhon J, Thurnauer M, Woloschak G (2003) *Nat Mater* 2:343
12. Cozzoli PD, Kornowski A, Weller H (2003) *J Am Chem Soc* 125:14539
13. Huynh WU, Dittmer JJ, Alivisatos AP (2002) *Science* 295:2427
14. Li J, Wang LW (2003) *Nano Lett* 3:1357
15. Lei Y, Zhang LD, Meng GW, Li GH, Zhang XY, Liang CH, Chen W, Wang SX (2001) *Appl Phys Lett* 78:1125
16. Zhang Q, Gao L (2003) *Langmuir* 19:967
17. Sugimoto T, Zhou X, Muramatsu A (2003) *J Colloid Interface Sci* 259:53
18. Sugimoto T (2003) *Chem Eng Technol* 26:313
19. Chemseddine A, Moritz T (1999) *Eur Inorg Chem* 1999:235
20. Trentler TJ, Denler TE, Bertone JF, Agrawal A, Colvin VL (1999) *J Am Chem Soc* 121:1613
21. Armstrong AR, Armstrong G, Canales J, Bruce PG (2004) *Angew Chem Int Ed* 43:2286
22. Jun Y, Casula MF, Sim JH, Kim SY, Cheon J, Alivisatos AP (2003) *J Am Chem Soc* 125:15981
23. Fieevet F, Lagier JP, Figlarz M (1989) *MRS Bull* 14:29
24. Sun Y, Xia Y (2002) *Adv Mater* 14:833
25. Wang Y, Jiang X, Xia Y (2003) *J Am Chem Soc* 125:16176
26. Jiang X, Wang Y, Herricks T, Xia Y (2004) *J Mater Chem* 14:695
27. Wang Y, Jiang X, Herricks T, Xia Y (2004) *J Phys Chem B* 108:8631
28. Jana NR (2004) *Angew Chem* 116:1562